

# Homoleptic Copper(I) and Silver(I) Complexes with *o*-Phenylene-Backboned Bis(thioethers), Bis(selenoethers), and Bis(telluroethers): Synthesis, Multinuclear NMR Studies, and Crystal Structures of $[\text{Cu}\{o\text{-C}_6\text{H}_4(\text{SeMe})_2\}_2]\text{PF}_6$ , $[\text{Cu}\{o\text{-C}_6\text{H}_4(\text{TeMe})_2\}_2]\text{PF}_6$ , and $[\text{Ag}_n\{\mu\text{-}o\text{-C}_6\text{H}_4(\text{SeMe})_2\}_n\{o\text{-C}_6\text{H}_4(\text{SeMe})_2\}_n][\text{BF}_4]_n \cdot n\text{CH}_2\text{Cl}_2$

Jane R. Black, Neil R. Champness, William Levason,\* and Gillian Reid

Department of Chemistry, University of Southampton, Southampton SO17 1BJ, U.K.

Received August 29, 1995<sup>⊗</sup>

Homoleptic copper(I) and silver(I) complexes  $[\text{M}(\text{L-L})_2]\text{X}$  ( $\text{M} = \text{Cu}$ ,  $\text{X} = \text{PF}_6$ ;  $\text{M} = \text{Ag}$ ,  $\text{X} = \text{BF}_4$ ;  $\text{L-L} = o\text{-C}_6\text{H}_4(\text{EMe})_2$ ;  $\text{E} = \text{S}$ ,  $\text{Se}$ ,  $\text{Te}$ ) have been prepared and characterized by analysis, FAB mass spectrometry, and multinuclear NMR spectroscopy ( $^1\text{H}$ ,  $^{77}\text{Se}$ ,  $^{125}\text{Te}$ ,  $^{63}\text{Cu}$ ,  $^{109}\text{Ag}$ ). Variable-temperature NMR studies have been used to probe various exchange processes occurring in solution. Single-crystal X-ray structural studies show that the Cu(I) complexes  $[\text{Cu}\{o\text{-C}_6\text{H}_4(\text{SeMe})_2\}_2]\text{PF}_6$  [trigonal,  $a = 13.29(2)$ ,  $c = 65.97(2)$  Å,  $R\bar{3}c$ ,  $Z = 18$ ] and  $[\text{Cu}\{o\text{-C}_6\text{H}_4(\text{TeMe})_2\}_2]\text{PF}_6$  [trigonal,  $a = 13.632(6)$  Å,  $c = 67.983(4)$  Å,  $R\bar{3}c$ ,  $Z = 18$ ] are isostructural and exist as mononuclear species with chelating bis(seleno- and bis(telluroethers), respectively, whereas the single-crystal structure of  $[\text{Ag}_n\{\mu\text{-}o\text{-C}_6\text{H}_4(\text{SeMe})_2\}_n\{o\text{-C}_6\text{H}_4(\text{SeMe})_2\}_n]^{n+}$ , discrete  $\text{BF}_4^-$ , anions and  $\text{CH}_2\text{Cl}_2$  solvent molecules. The  $o\text{-C}_6\text{H}_4(\text{SeMe})_2$  ligands in the latter exist as a mixture of invertomers within the infinite chains; the chelating ones adopt the *meso* arrangement while the bridging ones occur as the DL form. This is the first structurally characterized complex involving a bridging *o*-phenylene group 16 donor ligand and the first case of both invertomers occurring in a single complex.

## Introduction

We have recently reported the synthesis of a variety of homoleptic Ag(I) and Cu(I) complexes with bis(thioethers), bis(selenoethers), and bis(telluroethers) with alkane backbones  $\text{RE}(\text{CH}_2)_n\text{ER}$  ( $\text{R} = \text{Me}$ ,  $\text{Ph}$ ;  $\text{E} = \text{S}$ ,  $\text{Se}$ ,  $n = 1\text{--}3$ ;  $\text{E} = \text{Te}$ ,  $n = 1, 3$ ).<sup>1–3</sup> Single-crystal X-ray studies have shown that, in the solid state, while the complexes of  $\text{RE}(\text{CH}_2)_2\text{ER}$  contain chelating ligands, those with  $\text{RE}(\text{CH}_2)_3\text{ER}$  or  $\text{RECH}_2\text{ER}$  are ligand-bridged infinite polymers. The solution behavior of these complexes has been probed by variable-temperature multinuclear NMR ( $^1\text{H}$ ,  $^{77}\text{Se}$ ,  $^{125}\text{Te}$ ,  $^{63}\text{Cu}$ ,  $^{109}\text{Ag}$ ) spectroscopy, which revealed extreme lability with no spin–spin couplings or diastereoisomers (invertomers) observable even at the lowest temperatures studied (*ca.* 180 K). Here we report a similar investigation of the complexes with *o*-phenylene-backboned ligands,  $o\text{-C}_6\text{H}_4(\text{EMe})_2$ . The reasons for the present study were 4-fold: the rigid *o*-phenylene backbone is expected to reduce ligand dissociation (cf. the *o*-phenylene backbone effect in complexes of  $o\text{-C}_6\text{H}_4(\text{PMe}_2)_2$  or  $o\text{-C}_6\text{H}_4(\text{AsMe}_2)_2$ ),<sup>4,5</sup> which if slowed sufficiently with respect to the NMR timescales would allow metal–donor spin–spin couplings to be observed; reduced dissociation rates might similarly permit identification of invertomers; the alkane-backboned ligands show unusual *low-frequency* coordination shifts in the  $^{77}\text{Se}$  and  $^{125}\text{Te}$  NMR spectra, and the effects of backbone unsaturation on this are of interest; finally, the  $[\text{M}\{o\text{-C}_6\text{H}_4(\text{TeMe})_2\}_2]^+$  complexes ( $\text{M} = \text{Cu}$ ,  $\text{Ag}$ )

would be the first examples involving a five-membered chelate ring bis(telluroether) ( $\text{RTe}(\text{CH}_2)_2\text{TeR}$  cannot be made).<sup>6</sup>

## Experimental Section

Physical measurements were made as described elsewhere.<sup>1</sup>

Silver-109 NMR spectra were recorded on a Bruker AM360 spectrometer at 16.75 MHz. Spectra were obtained from solutions in  $\text{CH}_2\text{Cl}_2$  or  $\text{CH}_3\text{NO}_2$  containing 5% of the deuteriated analogue to provide the lock, in 10 mm o.d. tubes. Spectra were recorded by direct observation from solutions containing the free radical relaxation agent TEMPO (TANOL)<sup>8</sup> and with a 2 s pulse delay, typically 20 000 scans being accumulated. A 9.1 mol  $\text{dm}^{-3}$  solution of  $\text{AgNO}_3$  in  $\text{D}_2\text{O}$  containing  $\text{Fe}^{3+}$  as relaxation agent was used as zero reference.<sup>9</sup> This “zero” is +47 ppm from the  $\text{Ag}^+$  resonance at “infinite dilution”. Copper-63 NMR were recorded at 95.5 MHz also on a Bruker AM360 and referenced to  $[\text{Cu}(\text{MeCN})_4]^+$  (0 ppm) in MeCN at 300 K.

**Synthesis.** The complexes were prepared by the same general method described below. Complexes were made under a nitrogen atmosphere, and the silver samples were stored in sealed containers wrapped in aluminium foil in a freezer. Most of the silver complexes are light sensitive to some degree, and some darken rapidly in solution in diffuse daylight.

**Synthesis of  $[\text{Cu}(\text{L-L})_2]\text{PF}_6$  and  $[\text{Ag}(\text{L-L})_2]\text{BF}_4$ .** The copper complexes were prepared by addition of  $[\text{Cu}(\text{MeCN})_4]\text{PF}_6$  (1 mmol) to a solution of the ligand (2.1 mmol) in  $\text{CH}_2\text{Cl}_2$  (10  $\text{cm}^3$ ). The reaction mixture was refluxed for 10 min and then allowed to cool to room temperature. Diethyl ether (20  $\text{cm}^3$ ) was added to precipitate the product which was filtered off, washed with diethyl ether (3  $\times$  10  $\text{cm}^3$ ), and vacuum dried. Yields were *ca.* 80%. Anal. Calcd for  $\text{C}_{16}\text{H}_{20}$ -

<sup>⊗</sup> Abstract published in *Advance ACS Abstracts*, March 1, 1996.

- (1) Black, J. R.; Levason, W. *J. Chem. Soc., Dalton Trans.* **1994**, 3225.
- (2) Black, J. R.; Champness, N. R.; Levason, W.; Reid, G. *J. Chem. Soc., Chem. Commun.* **1995**, 1277. Black, J. R.; Champness, N. R.; Levason, W.; Reid, G. *J. Chem. Soc., Dalton Trans.* **1995**, 3439.
- (3) Black, J. R.; Champness, N. R.; Levason, W.; Reid, G. Manuscript in preparation.
- (4) Warren, L. F.; Bennett, M. A. *Inorg. Chem.* **1976**, *15*, 3126.
- (5) Levason, W. *Comments Inorg. Chem.* **1990**, *9*, 331.

- (6) Hope, E. G.; Kemmitt, T.; Levason, W. *Organometallics* **1988**, *7*, 78.
- (7) Endo, K.; Yamamoto, K.; Matsushita, K.; Deguchi, K.; Kanda, K.; Nakatsujii, H. *J. Magn. Reson.* **1985**, *65*, 268.
- (8) Burges, C. W.; Koschmieder, R.; Sahn, W.; Schwenk, A. *Z. Naturforsch., Sect. A* **1973**, *28A*, 1753.
- (9) PATTY: The DIRDIF program system. Beurskens, P. T.; Admiraal, G.; Beurskens, G.; Bosman, W. P.; Garcia-Granda, S.; Gould, R. O.; Smits, J. M. M.; Smykalla, C. University of Nijmegen, The Netherlands, 1992.

**Table 1.** Crystallographic Data<sup>a</sup>

complex formula	[Cu{ <i>o</i> -C <sub>6</sub> H <sub>4</sub> (SeMe) <sub>2</sub> }] <sub>2</sub> PF <sub>6</sub>	[Cu{ <i>o</i> -C <sub>6</sub> H <sub>4</sub> (TeMe) <sub>2</sub> }] <sub>2</sub> PF <sub>6</sub>	[Ag <sub>n</sub> { <i>μ</i> - <i>o</i> -C <sub>6</sub> H <sub>4</sub> (SeMe) <sub>2</sub> }] <sub>2n</sub> { <i>o</i> -C <sub>6</sub> H <sub>4</sub> (SeMe) <sub>2</sub> }] <sub>n</sub> (BF <sub>4</sub> ) <sub>n</sub> · <i>n</i> CH <sub>2</sub> Cl <sub>2</sub>
fw	736.7	931.2	1530.6
<i>T</i> /K	150	150	150
cryst syst	trigonal	trigonal	monoclinic
space group	<i>R</i> 3 <i>c</i>	<i>R</i> 3 <i>c</i>	<i>P</i> 2 <sub>1</sub> / <i>c</i>
<i>a</i> /Å	13.29(2)	13.632(6)	19.273(7)
<i>b</i> /Å	13.29(2)	13.632(6)	11.927(3)
<i>c</i> /Å	65.97(2)	67.983(4)	20.405(6)
α/deg	90	90	90
β/deg	90	90	90.42(3)
γ/deg	120	120	90
<i>V</i> /Å <sup>3</sup>	10 083(22)	10 940(2)	4690(2)
<i>Z</i>	18	18	4
<i>D</i> <sub>c</sub> /g cm <sup>-3</sup>	2.184	2.544	2.167
λ(Mo Kα)/Å	0.710 73	0.710 73	0.710 73
μ(Mo Kα)/cm <sup>-1</sup>	75.94	57.15	72.12
GOF	2.10	1.67	2.34
<i>R</i> ( <i>F</i> <sub>o</sub> )	0.040	0.025	0.045
<i>R</i> <sub>w</sub> ( <i>F</i> <sub>o</sub> )	0.039	0.029	0.051

$$^a R = \sum_{i=1}^n (|F_{o,i}| - |F_{c,i}|) / \sum_{i=1}^n |F_{o,i}|. R_w = [\sum_{i=1}^n w_i (|F_{o,i}| - |F_{c,i}|)^2 / \sum_{i=1}^n w_i |F_{o,i}|^2]^{1/2}. GOF = [\sum_{i=1}^n (|F_{o,i}| - |F_{c,i}|) / \sigma_i] / (n - m) \cong 1.$$

CuF<sub>6</sub>PS<sub>4</sub>: C, 35.0; H, 3.7. Found: C, 34.7; H, 3.7. Calcd for C<sub>16</sub>H<sub>20</sub>CuF<sub>6</sub>PS<sub>4</sub>: C, 26.1; H, 2.7. Found: C, 25.5; H, 2.2. Calcd for C<sub>16</sub>H<sub>20</sub>CuF<sub>6</sub>PTe<sub>4</sub>: C, 20.6; H, 2.2. Found: C, 20.6; H, 1.9.

The silver complexes were prepared by addition of the ligand (2.1 mmol) to a solution of anhydrous AgBF<sub>4</sub> (1 mmol) in acetone (10 cm<sup>3</sup>). Ice cold diethyl ether was added to precipitate the product, which was filtered off, washed with diethyl ether (3 × 10 cm<sup>3</sup>), and vacuum dried. Yields were 70–80%. Anal. Calcd for C<sub>16</sub>H<sub>20</sub>AgBF<sub>4</sub>S<sub>4</sub>: C, 35.9; H, 3.8. Found: C, 35.9; H, 4.0. Calcd for C<sub>16</sub>H<sub>20</sub>AgBF<sub>4</sub>Se<sub>4</sub>: C, 26.6; H, 2.8. Found: C, 26.7; H, 2.2. Calcd for C<sub>16</sub>H<sub>20</sub>AgBF<sub>4</sub>Te<sub>4</sub>: C, 21.0; H, 2.2. Found: C, 21.4; H, 2.3.

**X-ray Crystallographic Studies.** Crystallographic data are given in Table 1 for the three structures. In each case the selected crystal was coated with mineral oil and mounted on a glass fiber. Data collection used a Rigaku AFC7S four-circle diffractometer equipped with an Oxford Cryostreams low-temperature attachment, using graphite-monochromated Mo Kα X-radiation. The intensities of three standard reflections were measured after every 150 data. The structures were each solved by heavy atom Patterson methods<sup>9</sup> and developed by using iterative cycles of full-matrix least-squares refinement and difference Fourier syntheses which located all non-H atoms in the asymmetric unit.<sup>10</sup> The weighting scheme  $w^{-1} = \sigma^2(F)$  gave satisfactory agreement in each case.

[Cu{*o*-C<sub>6</sub>H<sub>4</sub>(TeMe)<sub>2</sub>}]<sub>2</sub>PF<sub>6</sub>. No significant crystal decay or movement was observed. As there were no identifiable faces, the data were corrected for absorption using  $\psi$ -scans. This compound crystallizes in a trigonal space group, and the asymmetric unit comprises one-half [Cu{*o*-C<sub>6</sub>H<sub>4</sub>(TeMe)<sub>2</sub>}]<sub>2</sub><sup>+</sup> cation in which the Cu(I) ion occupies a site of 2-fold crystallographic symmetry (*x*, *x*, 0.25) (this 2-fold operation generates the full cation), one 1/3 occupied PF<sub>6</sub><sup>-</sup> anion [P(1) occupies a crystallographic 3-fold site, (1, 0, *z*), with two fully occupied F atoms, F(1) and F(2)], and one 1/6 occupied PF<sub>6</sub><sup>-</sup> anion [P(2) occupies a crystallographic 6-fold site, (1, 0, 0.5), with one fully occupied F atom]. All non-H atoms were refined anisotropically, while H-atoms were included in fixed, calculated positions. Selected bond lengths and angles are listed in Table 2.

[Cu{*o*-C<sub>6</sub>H<sub>4</sub>(SeMe)<sub>2</sub>}]<sub>2</sub>PF<sub>6</sub>. This was a rather poor quality crystal which gave only relatively weak data; hence, the data set is slightly truncated, with the final shell at high angle, 45 < 2θ < 50°, being terminated before completion. During data collection the intensities of the standard reflections decreased by 9.1%. A linear correction factor was applied to the data to take account of this. This compound is isostructural with [Cu{*o*-C<sub>6</sub>H<sub>4</sub>(TeMe)<sub>2</sub>}]<sub>2</sub>PF<sub>6</sub>, crystallizing in the same trigonal space group and with very similar unit cell parameters. Similar fragments are also observed in the asymmetric unit. At isotropic convergence the data were corrected for absorption using DIFABS,<sup>11</sup>

**Table 2.** Selected Bond Lengths (Å) and Angles (deg) for [Cu{*o*-C<sub>6</sub>H<sub>4</sub>(TeMe)<sub>2</sub>}]<sub>2</sub><sup>+</sup>

Bond Lengths			
Te(1)–Cu(1)	2.5598(7)	Te(1)–C(1)	2.130(7)
Te(1)–C(2)	2.112(6)	Te(2)–Cu(1)	2.5299(8)
Te(2)–C(7)	2.141(6)	Te(2)–C(8)	2.134(7)
C(2)–C(3)	1.401(8)	C(2)–C(7)	1.392(8)
C(3)–C(4)	1.390(9)	C(4)–C(5)	1.37(1)
C(5)–C(6)	1.397(9)	C(6)–C(7)	1.391(8)
Bond Angles			
Cu(1)–Te(1)–C(1)	106.1(2)	Cu(1)–Te(1)–C(2)	98.3(2)
C(1)–Te(1)–C(2)	94.7(2)	Cu(1)–Te(2)–C(7)	97.8(2)
Cu(1)–Te(2)–C(8)	105.9(2)	C(7)–Te(2)–C(8)	96.6(2)
Te(1)–Cu(1)–Te(1)	111.65(4)	Te(1)–Cu(1)–Te(2)	112.31(1)
Te(1)–Cu(1)–Te(2)	95.59(1)	Te(2)–Cu(1)–Te(2)	129.74(5)
Te(1)–C(2)–C(3)	116.4(4)	Te(1)–C(2)–C(7)	123.6(4)
C(3)–C(2)–C(7)	120.0(6)	C(2)–C(3)–C(4)	119.9(6)
C(3)–C(4)–C(5)	120.0(6)	C(4)–C(5)–C(6)	120.6(6)
C(5)–C(6)–C(7)	119.9(6)	Te(2)–C(7)–C(2)	124.4(4)
Te(2)–C(7)–C(6)	115.8(5)	C(2)–C(7)–C(6)	119.6(6)

which resulted in reduced residual electron density, R-factors, and esd's on the atomic positions. All non-H atoms, except for the Cu atom, were then refined anisotropically, while H atoms were included in fixed, calculated positions. Attempts to refine atom Cu(1) with anisotropic thermal parameters resulted in an unsatisfactory thermal ellipsoid and a significant increase in the R-factor and esd's on the atomic positions. This effect may be due to the rather poor quality of the crystals available and correspondingly relatively poor data. However, since the structure of this complex was clearly established and isostructural with the telluroether analogue, it was not considered necessary to recollect data on another sample. Selected bond lengths and angles are listed in Table 3.

[Ag<sub>n</sub>{*μ*-*o*-C<sub>6</sub>H<sub>4</sub>(SeMe)<sub>2</sub>}]<sub>2n</sub>{*o*-C<sub>6</sub>H<sub>4</sub>(SeMe)<sub>2</sub>}]<sub>n</sub>(BF<sub>4</sub>)<sub>n</sub>·*n*CH<sub>2</sub>Cl<sub>2</sub>. During data collection no significant crystal decay or movement was observed. As there were no identifiable faces, the data were corrected for absorption using  $\psi$ -scans. The unit cell comprises a dinuclear [Ag<sub>2</sub>{*μ*-*o*-C<sub>6</sub>H<sub>4</sub>(SeMe)<sub>2</sub>}]<sub>2</sub>{*o*-C<sub>6</sub>H<sub>4</sub>(SeMe)<sub>2</sub>}]<sub>2</sub><sup>2+</sup> cationic repeating fragment, two discrete BF<sub>4</sub><sup>-</sup> anions, and a CH<sub>2</sub>Cl<sub>2</sub> solvent molecule. During refinement some disorder was identified in the BF<sub>4</sub><sup>-</sup> anions. This was modeled successfully by using partial F atom occupancies; the partial F atoms refined to 50% occupancy. Thus, around B(1) there are two fully occupied F atoms, F(1) and F(2), and four 50% occupied F atoms, F(3)–F(6), while B(2) has eight 50% occupied F atoms surrounding it, F(9)–(14). All non-H atoms, except for the partially occupied F atoms, were refined anisotropically, while H atoms were included in fixed, calculated positions. Selected bond lengths and angles are listed in Table 4.

(10) TeXsan: Crystal Structure Analysis Package, Molecular Structure Corp., 1992.

(11) Walker, N.; Stuart, D. *Acta Crystallogr., Sect. A* **1983**, 39, 158.

**Table 3.** Selected Bond Lengths (Å) and Angles (deg) for  $[\text{Cu}\{o\text{-C}_6\text{H}_4(\text{SeMe})_2\}_2]^+$ 

Bond Lengths			
Se(1)—Cu(1)	2.419(2)	Se(1)—C(1)	1.96(1)
Se(1)—C(2)	1.905(10)	Se(2)—Cu(1)	2.379(2)
Se(2)—C(7)	1.93(1)	Se(2)—C(8)	1.92(1)
C(2)—C(3)	1.41(1)	C(2)—C(7)	1.39(1)
C(3)—C(4)	1.39(2)	C(4)—C(5)	1.39(2)
C(5)—C(6)	1.38(2)	C(6)—C(7)	1.42(1)
Bond Angles			
Cu(1)—Se(1)—C(1)	106.5(4)	Cu(1)—Se(1)—C(2)	99.2(3)
C(1)—Se(1)—C(2)	96.2(4)	Cu(1)—Se(2)—C(7)	99.0(3)
Cu(1)—Se(2)—C(8)	108.3(4)	C(7)—Se(2)—C(8)	99.3(5)
Se(1)—Cu(1)—Se(1)	114.05(10)	Se(1)—Cu(1)—Se(2)	113.19(7)
Se(1)—Cu(1)—Se(2)	94.20(7)	Se(2)—Cu(1)—Se(2)	129.2(1)
Se(1)—C(2)—C(3)	117.8(8)	Se(1)—C(2)—C(7)	123.3(8)
C(3)—C(2)—C(7)	118.8(10)	C(2)—C(3)—C(4)	121(1)
C(3)—C(4)—C(5)	119(1)	C(4)—C(5)—C(6)	120(1)
C(5)—C(6)—C(7)	120(1)	Se(2)—C(7)—C(2)	124.1(8)
Se(2)—C(7)—C(6)	116.3(8)	C(2)—C(7)—C(6)	119(1)

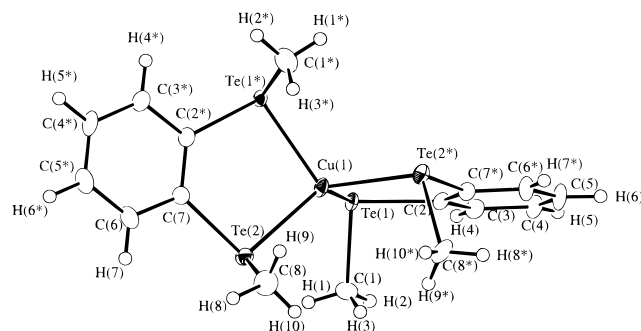
**Table 4.** Selected Bond Lengths (Å) and Angles (deg) for  $[\text{Ag}_n\{\mu\text{-}o\text{-C}_6\text{H}_4(\text{SeMe})_2\}_n\{o\text{-C}_6\text{H}_4(\text{SeMe})_2\}_n]^{n+}$ 

Bond Lengths			
Ag(1)—Se(1)	2.681(2)	Ag(1)—Se(2)	2.708(1)
Ag(1)—Se(3)	2.596(1)	Ag(1)—Se(4)	2.703(1)
Ag(2)—Se(5)	2.673(1)	Ag(2)—Se(6)	2.861(1)
Ag(2)—Se(7)	2.658(2)	Ag(2)—Se(8)	2.587(1)
Se(1)—C(1)	1.94(1)	Se(1)—C(2)	1.938(10)
Se(2)—C(7)	1.92(1)	Se(2)—C(8)	1.96(1)
Se(3)—C(9)	1.95(1)	Se(3)—C(10)	1.95(1)
Se(4)—C(12)	1.92(1)	Se(4)—C(13)	1.93(1)
Se(5)—C(18)	1.928(9)	Se(5)—C(19)	1.95(1)
Se(6)—C(20)	1.94(1)	Se(6)—C(21)	1.92(1)
Se(7)—C(26)	1.93(1)	Se(7)—C(27)	1.95(1)
Se(8)—C(28)	1.92(1)	Se(8)—C(29)	1.94(1)
Bond Angles			
Se(1)—Ag(1)—Se(2)	79.64(4)	Se(1)—Ag(1)—Se(3)	118.92(5)
Se(1)—Ag(1)—Se(4)	115.51(5)	Se(2)—Ag(1)—Se(3)	128.67(5)
Se(2)—Ag(1)—Se(4)	102.68(4)	Se(3)—Ag(1)—Se(4)	108.76(4)
Se(5)—Ag(2)—Se(6)	113.88(4)	Se(5)—Ag(2)—Se(7)	106.62(5)
Se(5)—Ag(2)—Se(8)	119.40(4)	Se(6)—Ag(2)—Se(7)	73.75(5)
Se(6)—Ag(2)—Se(8)	104.66(5)	Se(7)—Ag(2)—Se(8)	128.58(5)
Ag(1)—Se(1)—C(1)	102.1(4)	Ag(1)—Se(1)—C(2)	97.0(3)
Ag(2)—Se(7)—C(26)	94.4(3)	Ag(2)—Se(7)—C(27)	101.8(4)
C(26)—Se(7)—C(27)	99.8(6)	Ag(2)—Se(8)—C(28)	101.7(3)
Ag(2)—Se(8)—C(29)	99.9(3)	C(28)—Se(8)—C(29)	100.5(4)
C(1)—Se(1)—C(2)	99.0(5)	Ag(1)—Se(2)—C(7)	97.1(3)
Ag(1)—Se(2)—C(8)	101.4(3)	C(7)—Se(2)—C(8)	98.9(4)
Ag(1)—Se(3)—C(9)	101.7(3)	Ag(1)—Se(3)—C(10)	103.6(3)
C(9)—Se(3)—C(10)	99.7(5)	Ag(1)—Se(4)—C(12)	99.3(5)
Ag(1)—Se(4)—C(13)	93.4(3)	C(12)—Se(4)—C(13)	100.9(5)
Ag(2)—Se(5)—C(18)	84.6(3)	Ag(2)—Se(5)—C(19)	102.5(3)
C(18)—Se(5)—C(19)	101.4(5)	Ag(2)—Se(6)—C(20)	115.1(4)
Ag(2)—Se(6)—C(21)	91.3(3)	C(20)—Se(6)—C(21)	99.6(5)

Additional material available from the Cambridge Crystallographic Data Centre comprises H atom coordinates, thermal parameters, and full listings of bond lengths and angles for the three structures.

## Results and Discussion

The synthesis of the complexes was straightforward, affording white (bis(thioether) and bis(selenoether)) or yellow (bis(telluroether)) powders. The silver complexes darken slowly on exposure to light. The  $[\text{Ag}\{o\text{-C}_6\text{H}_4(\text{TeMe})_2\}_2]\text{BF}_4$  complex was poorly soluble in  $\text{CH}_2\text{Cl}_2$ ,  $\text{CHCl}_3$ , or  $\text{MeCN}$  but was more soluble in  $\text{MeNO}_2$  or  $\text{HCONMe}_2$ , although in these the complex decomposed slowly even in the dark, depositing a fine black powder. The other complexes were easily soluble in all the above solvents. The FAB mass spectra of all six complexes (3-NOBA matrix) showed  $[\text{M}(\text{L-L})_2]^+$  and  $[\text{M}(\text{L-L})]^+$  as the

**Figure 1.** View of the structure of  $[\text{Cu}\{o\text{-C}_6\text{H}_4(\text{TeMe})_2\}_2]^+$  with numbering scheme adopted. Ellipsoids are drawn at 40% probability.

major ions with no peaks corresponding to dimetallic species, although the X-ray structure (below) showed that the  $[\text{Ag}\{o\text{-C}_6\text{H}_4(\text{SeMe})_2\}_2]\text{BF}_4$  was a ligand-bridged polymer in the solid state. Similar behavior was also observed for complexes of  $\text{RE}(\text{CH}_2)_3\text{ER}$  ligands,<sup>1,2</sup> which are also polymeric. This presumably reflects rearrangement of these labile complexes in the matrix and shows that the absence of di- or poly-metallic ions in their FAB mass spectra does not allow one to infer chelated monomer structures for the solids.

**X-ray Crystal Structures.** Crystals of suitable quality for single-crystal X-ray diffraction studies were grown for the two copper complexes at  $-20^\circ\text{C}$  by layering  $\text{CH}_2\text{Cl}_2$  solutions with ethanol and for the silver bis(selenoether) complex by vapor diffusion of diethyl ether into a  $\text{CH}_2\text{Cl}_2$  solution of the complex. Repeated attempts to obtain crystals of the silver bis(telluroether) complex foundered on the poor solution stability of this material. In contrast several batches of crystals of both the copper and silver bis(thioether) complexes were produced from ethanol/ $\text{CH}_2\text{Cl}_2$  but on examination all proved to be twinned.

The crystal structure of  $[\text{Cu}\{o\text{-C}_6\text{H}_4(\text{TeMe})_2\}_2]^+$  shows (Figure 1) tetrahedrally coordinated Cu(I) ions bonded to two chelating  $o\text{-C}_6\text{H}_4(\text{TeMe})_2$  ligands giving discrete mononuclear cations, with  $\text{Cu}(1)\text{—Te}(1) = 2.5598(7)$  and  $\text{Cu}(1)\text{—Te}(2) = 2.5299(8)$  Å. This is the first structurally characterized example of a telluroether complex involving five-membered chelate rings.<sup>12</sup> The Te—Cu—Te angles involved in the five-membered chelate rings are significantly smaller than the  $109^\circ$  expected for a regular tetrahedron, reflecting the restricted bite angle of the *o*-phenylene bis(telluroether) ligand. The overall geometry is therefore a distorted, flattened tetrahedron. This telluroether complex is isostructural with the selenoether analogue,  $[\text{Cu}\{o\text{-C}_6\text{H}_4(\text{SeMe})_2\}_2]\text{PF}_6$ , which shows (Figure 2) tetrahedrally coordinated Cu(I) ions bonded to four Se donors from the two chelating bis(selenoether) ligands, with  $\text{Cu}(1)\text{—Se}(1) = 2.419(2)$  and  $\text{Cu}(1)\text{—Se}(2) = 2.379(2)$  Å. These Cu—Se distances compare well with those reported for other selenoether complexes, e.g.  $[\text{Cu}_n(\text{MeSeCH}_2\text{SeMe})_{2n}]^{n+}$ ,  $d(\text{Cu—Se}) = 2.40\text{—}2.46$  Å,<sup>3</sup> and  $[\text{Cu}(\text{16janeSe}_4)](\text{SO}_3\text{CF}_3)$  ( $16\text{janeSe}_4 = 1,5,9,13\text{-tetraselenacyclohexadecane}$ ),  $d(\text{Cu—Se}) = 2.42\text{—}2.52$  Å.<sup>13</sup> The angles around the central Cu atom in  $[\text{Cu}\{o\text{-C}_6\text{H}_4(\text{SeMe})_2\}_2]^+$  show deviations from tetrahedral geometry similar to those observed for  $[\text{Cu}\{o\text{-C}_6\text{H}_4(\text{TeMe})_2\}_2]^+$ . The *o*-phenylene bis(telluroether) and bis(selenoether) ligands in these complexes adopt a *meso* configuration, with both Me groups on each ligand directed to the same side of the plane defined by the aromatic ring.

A single-crystal X-ray analysis of the corresponding 1:2 metal: $o\text{-C}_6\text{H}_4(\text{SeMe})_2$  complex incorporating Ag(I),  $[\text{Ag}\{o\text{-C}_6\text{H}_4(\text{SeMe})_2\}_2]^+$

(12) Hope, E. G.; Levason, W. *Coord. Chem. Rev.* **1993**, *122*, 109.

(13) Batchelor, R. J.; Einstein, F. W. B.; Gay, I. D.; Gu, J. H.; Pinto, B. M. *J. Organomet. Chem.* **1991**, *411*, 376.

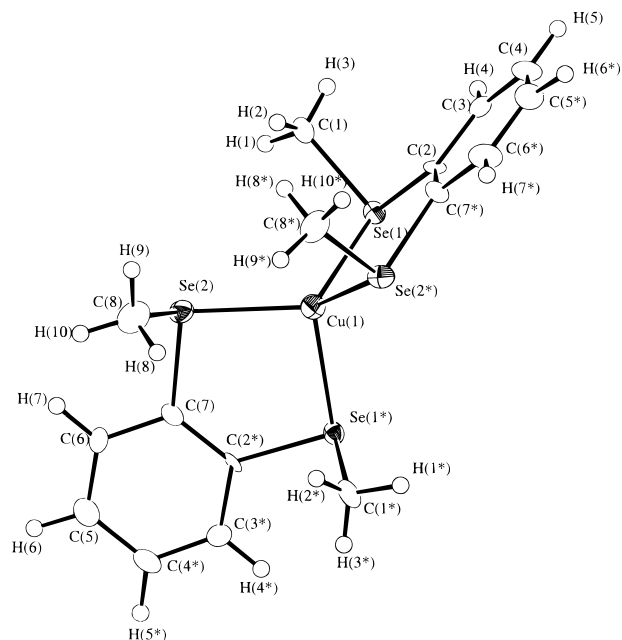


**Figure 2.** View of the structure of  $[\text{Cu}\{\text{o-C}_6\text{H}_4(\text{SeMe})_2\}_2]^+$  with numbering scheme adopted. Ellipsoids are drawn at 40% probability.

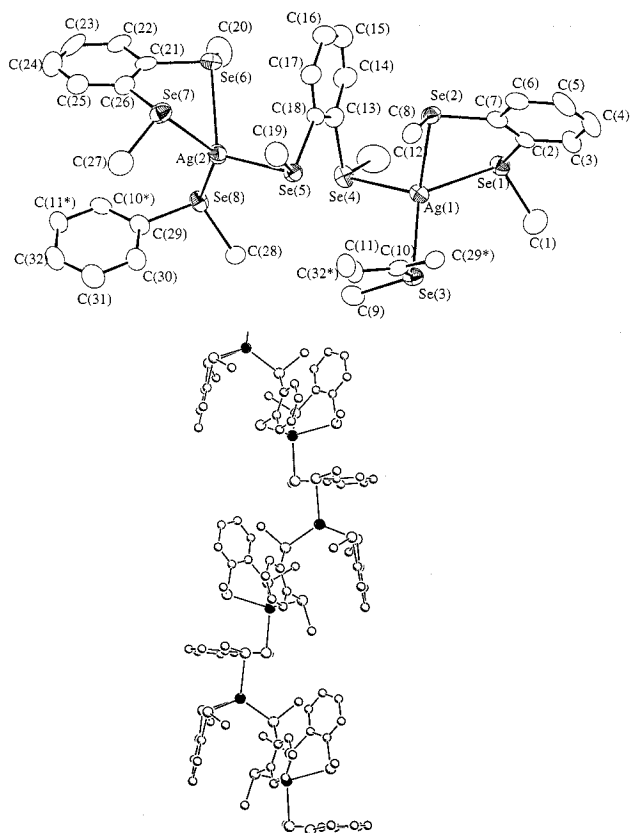


**Figure 3.** (a) View of the dinuclear  $[\text{Ag}_2\{\mu\text{-o-C}_6\text{H}_4(\text{SeMe})_2\}_2\{\text{o-C}_6\text{H}_4(\text{SeMe})_2\}_2]^{2+}$  repeating unit in the asymmetric unit with numbering scheme adopted. Ellipsoids are drawn at 40% probability. (b) View down the *a*-axis of the cationic chain polymer,  $[\text{Ag}_n\{\mu\text{-o-C}_6\text{H}_4(\text{SeMe})_2\}_n\{\text{o-C}_6\text{H}_4(\text{SeMe})_2\}_n]^{n+}$  (Ag atoms are shaded).

$\text{C}_6\text{H}_4(\text{SeMe})_2\}_2]\text{BF}_4$ , reveals a very different arrangement from the Cu(I) analogue. The structure shows (Figure 3a,b) infinite chains of  $[\text{Ag}_n\{\mu\text{-o-C}_6\text{H}_4(\text{SeMe})_2\}_n\{\text{o-C}_6\text{H}_4(\text{SeMe})_2\}_n]^{n+}$  cations with discrete  $\text{BF}_4^-$  anions maintaining electroneutrality. Each Ag(I) atom coordinates to both Se-donors of one chelating bis(selenoether) and to one Se-donor of each of two bridging bis(selenoethers). One of the bridging ligands then links to the

**Table 5.**  $^1\text{H}$  NMR Data

complex	$\delta/\text{ppm}^a$
$[\text{Cu}\{\text{o-C}_6\text{H}_4(\text{SMe})_2\}_2]\text{PF}_6$	2.74 (s, 6H), 7.50–7.90 (m, 4H)
$[\text{Cu}\{\text{o-C}_6\text{H}_4(\text{SeMe})_2\}_2]\text{PF}_6$	2.62 (s, 6H), ( $^2J_{\text{Se-H}} = 9.5$ Hz), 7.47–8.0 (m, 4H)
$[\text{Cu}\{\text{o-C}_6\text{H}_4(\text{TeMe})_2\}_2]\text{PF}_6$	2.38 (s, 6H), 7.40–8.10 (m, 4H)
$[\text{Ag}\{\text{o-C}_6\text{H}_4(\text{SMe})_2\}_2]\text{PF}_4$	2.60 (s, 6H), 7.35–7.54 (m, 4H)
$[\text{Ag}\{\text{o-C}_6\text{H}_4(\text{SeMe})_2\}_2]\text{BF}_4$	2.58 (s, 6H) ( $^2J_{\text{Se-H}} \approx 10$ Hz), 7.37–7.85 (m, 4H)
$[\text{Ag}\{\text{o-C}_6\text{H}_4(\text{TeMe})_2\}_2]\text{BF}_4^b$	2.32 (s, 6H), 7.27–8.10 (m, 4H)

<sup>a</sup> In  $\text{CD}_2\text{Cl}_2$ , at 300 K unless indicated otherwise. <sup>b</sup>  $\text{CD}_3\text{CN}$ .

adjacent Ag atom above, while the other links to the Ag atom below. Each Ag atom is therefore four-coordinate to a distorted tetrahedral array of Se atoms. The Ag–Se bond lengths lie within the range 2.59–2.86 Å. The range of bond lengths is greater than observed in other silver(I) selenoether complexes, e.g.  $[\text{Ag}_n(\text{PhSeCH}_2\text{CH}_2\text{CH}_2\text{SePh})_{2n}]^{n+}$ ,  $d(\text{Ag-Se}) = 2.643\text{--}2.695$  Å,<sup>1</sup> and  $[\text{Ag}(\text{MeSeCH}_2\text{CH}_2\text{SeMe})_2]^{n+}$ ,  $d(\text{Ag-Se}) = 2.610\text{--}2.638$  Å.<sup>3</sup> Interestingly, the  $[\text{Ag}_n\{\mu\text{-o-C}_6\text{H}_4(\text{SeMe})_2\}_n\{\text{o-C}_6\text{H}_4(\text{SeMe})_2\}_n]^{n+}$  polymer involves different stereoisomeric forms of the *o*- $\text{C}_6\text{H}_4(\text{SeMe})_2$  unit. The chelating ligands adopt the *meso* configuration, while the bridging ligands adopt the *DL* form. This is the first structurally characterized example where *both* isomeric forms of a coordinated bis(thioether), bis(selenoether), or bis(telluroether) ligand have been observed in one species.<sup>12</sup> It is also a very rare example of bridging behavior by an *o*-phenylene-backboned bidentate ligand.

**Multinuclear NMR Studies.** The NMR data are summarized in Tables 5–7. The  $^1\text{H}$  NMR data (Table 5) are relatively uninformative exhibiting single  $\delta(\text{Me})$  resonances with small shifts from the free ligand values. Single methyl resonances were also observed on addition of free ligand at 300 K, demonstrating fast exchange. Even when the  $\text{CD}_2\text{Cl}_2$  solution of  $[\text{Cu}\{\text{o-C}_6\text{H}_4(\text{TeMe})_2\}_2]\text{PF}_6$  containing added ligand was cooled to 170 K, a single Me resonance was still observed.

The  $^{77}\text{Se}\{^1\text{H}\}$  and  $^{125}\text{Te}\{^1\text{H}\}$  spectra of the appropriate complexes proved much more informative (Table 6). At 300 K only single resonances were seen and little change in  $\delta$  occurred on cooling the solutions. All copper(I) and silver(I) complexes of  $\text{RE}(\text{CH}_2)_n\text{ER}$  ligands we have examined<sup>1–3</sup> exhibited unusual *low-frequency* coordination shifts, but as can be seen from Table 6, the coordination shifts in  $[\text{Cu}\{\text{o-C}_6\text{H}_4(\text{SeMe})_2\}_2]\text{PF}_6$ ,  $[\text{Cu}\{\text{o-C}_6\text{H}_4(\text{TeMe})_2\}_2]\text{PF}_6$ , and  $[\text{Ag}\{\text{o-C}_6\text{H}_4(\text{TeMe})_2\}_2]\text{BF}_4$  are to *high frequency*. Anomalously, that in  $[\text{Ag}\{\text{o-C}_6\text{H}_4(\text{SeMe})_2\}_2]\text{BF}_4$  is to *low frequency*. The interaction of the “free” lone pair on each coordinated Se or Te center with the delocalized aromatic system could be the source of the anomalous coordination shifts; such interactions are likely to be subtly dependent upon the orientation of the substituents with respect to the plane of the benzene rings. Although single resonances were observed at 300 K in the presence of the appropriate added free ligand, on cooling exchange slowed, and separate resonances for free and bound ligand were clearly resolved below *ca.* 210 K for the bis(selenoether) complexes and below *ca.* 240 K for  $[\text{Cu}\{\text{o-C}_6\text{H}_4(\text{TeMe})_2\}_2]\text{PF}_6$ . The poor solubility of  $[\text{Ag}\{\text{o-C}_6\text{H}_4(\text{TeMe})_2\}_2]\text{BF}_4$  in chlorocarbons prevented low temperature studies. Uniquely the  $^{125}\text{Te}\{^1\text{H}\}$  spectrum of  $[\text{Cu}\{\text{o-C}_6\text{H}_4(\text{TeMe})_2\}_2]\text{PF}_6$  below *ca.* 220 K resolved into several resonances (Figure 4). These resonances cannot be due to couplings to  $^{63/65}\text{Cu}$  for which two overlapping 1:1:1:1 quartets would be expected,<sup>14</sup> and we attribute them to

(14) Granger, P. In *Transition Metal NMR*; Pregosin, P. S., Ed.; Elsevier: Amsterdam, 1991; p 265. Black, J. R.; Levason, W.; Spicer, M. D.; Webster, M. *J. Chem. Soc., Dalton Trans.* **1993**, 3129.

**Table 6.**  $^{77}\text{Se}$  and  $^{125}\text{Te}$  NMR Data

complex	$\delta(^{77}\text{Se}$ or $^{125}\text{Te})/\text{ppm}^{b,c}$	comment
$[\text{Cu}\{o\text{-C}_6\text{H}_4(\text{SeMe})_2\}_2]\text{PF}_6$	+214 (300 K), +216 (180 K)	fast exchange with added ligand > ca. 210 K
$[\text{Ag}\{o\text{-C}_6\text{H}_4(\text{SeMe})_2\}_2]\text{BF}_4$	+180 (300 K), +180 (180 K)	fast exchange with added ligand > ca. 210 K
$[\text{Cu}\{o\text{-C}_6\text{H}_4(\text{TeMe})_2\}_2]\text{PF}_6$	+506 (300 K), ca. +515 (180 K)	several resonances resolve < ca. 220 K; fast exchange with added ligand > 240 K
$[\text{Ag}\{o\text{-C}_6\text{H}_4(\text{TeMe})_2\}_2]\text{BF}_4^d$	+433 (300 K), +432 (245 K)	fast exchange with added ligand down to mp of solvent

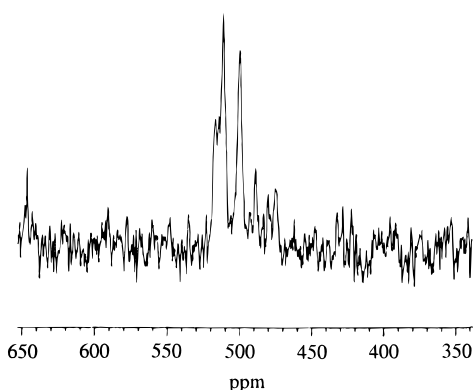
<sup>a</sup>  $^{77}\text{Se}$ ,  $I = 1/2$ , 7.58%,  $D_c = 2.98$ ;  $^{125}\text{Te}$ ,  $I = 1/2$ , 6.99%,  $D_c = 12.5$ . Recorded in  $\text{CH}_2\text{Cl}_2/\text{CD}_2\text{Cl}_2$  unless otherwise stated. <sup>b</sup> Relative to external neat  $\text{Me}_2\text{Se}$  or  $\text{Me}_2\text{Te}$  at 300 K. <sup>c</sup>  $o\text{-C}_6\text{H}_4(\text{SeMe})_2$ ,  $\delta = 200$ ;  $o\text{-C}_6\text{H}_4(\text{TeMe})_2$ ,  $\delta = +376$ . <sup>d</sup>  $\text{MeNO}_2/\text{CD}_3\text{NO}_2$ .

**Table 7.**  $^{63}\text{Cu}$  and  $^{109}\text{Ag}$  NMR Data

complex <sup>a</sup>	$\delta(^{63}\text{Cu}$ or $^{109}\text{Ag})/\text{ppm}^b$	comment
$[\text{Cu}\{o\text{-C}_6\text{H}_4(\text{SMe})_2\}_2]\text{PF}_6$		no resonances obsd 300–180 K or with added ligand
$[\text{Cu}\{o\text{-C}_6\text{H}_4(\text{SeMe})_2\}_2]\text{PF}_6$		no resonance obsd 300–180 K or with added ligand
$[\text{Cu}\{o\text{-C}_6\text{H}_4(\text{TeMe})_2\}_2]\text{PF}_6$	−109 ( $w_{1/2} = 4500$ Hz)	resonance broadens on cooling, disappears < ca. 240 K
$[\text{Ag}\{o\text{-C}_6\text{H}_4(\text{SMe})_2\}_2]\text{BF}_4$	+788 (300 K), +846 (180 K)	+803 (300 K), +848 (180 K) with added L-L
$[\text{Ag}\{o\text{-C}_6\text{H}_4(\text{SeMe})_2\}_2]\text{BF}_4$	+912 (300 K)	+867 with excess L-L
$[\text{Ag}\{o\text{-C}_6\text{H}_4(\text{TeMe})_2\}_2]\text{BF}_4^c$	+1128 (300 K)	+1164 (300 K) with added ligand

<sup>a</sup> Recorded in  $\text{CH}_2\text{Cl}_2/\text{CD}_2\text{Cl}_2$  unless otherwise stated.  $^{63}\text{Cu}$ ,  $I = 3/2$ , 69%;  $\Xi = 26.528$  MHz,  $D_c = 365$ , quadrupole moment  $-0.211 \times 10^{-28}$  m<sup>2</sup>;  $^{65}\text{Cu}$ ,  $I = 3/2$ , 31%,  $\Xi = 28.417$  MHz,  $D_c = 201$ , quadrupole moment  $-0.195 \times 10^{-28}$  m<sup>2</sup>;  $^{109}\text{Ag}$ ,  $I = 1/2$ , 48.2%,  $\Xi = 4.653$ ,  $D_c = 0.276$ .

<sup>b</sup> Relative to  $[\text{Cu}(\text{MeCN})_4]\text{BF}_4$  in MeCN at 300 K or 9.1 mol dm<sup>-3</sup> solution of  $\text{Ag}^+$  in  $\text{H}_2\text{O}/\text{D}_2\text{O}$ .

**Figure 4.**  $^{125}\text{Te}\{^1\text{H}\}$  NMR spectrum of  $[\text{Cu}\{o\text{-C}_6\text{H}_4(\text{TeMe})_2\}_2]\text{PF}_6$  in  $\text{CH}_2\text{Cl}_2$  at 180 K.

the different invertomers.<sup>15</sup> Pyramidal inversion rates are very sensitive to the metal center,<sup>16</sup> and this is the first observation of invertomers in a group 11 metal complex.<sup>1</sup>

Of the three copper complexes, only  $[\text{Cu}\{o\text{-C}_6\text{H}_4(\text{TeMe})_2\}_2]\text{PF}_6$  exhibited a  $^{63}\text{Cu}$  NMR resonance and then only over a limited temperature range (Table 7). The resonance of the quadrupolar  $^{63}\text{Cu}$  nucleus is only observable when quadrupolar relaxation is slow, in effect in environments approaching cubic symmetry; fast ligand dissociation or distorted environments cause the resonance to be unobservably broad.<sup>14</sup> The  $^{109}\text{Ag}$  NMR resonances were observed for all three complexes (Table 7), although the combination of long relaxation time, poor sensitivity, and low resonance frequency makes this a relatively difficult nucleus to study. The observed chemical shifts of the  $[\text{Ag}\{o\text{-C}_6\text{H}_4(\text{TeMe})_2\}_2]\text{BF}_4$  and  $[\text{Ag}\{o\text{-C}_6\text{H}_4(\text{SeMe})_2\}_2]\text{BF}_4$  are similar to those observed in  $\text{AgSe}/\text{Te}_4$  species,<sup>2</sup> but that of  $[\text{Ag}\{o\text{-C}_6\text{H}_4(\text{SMe})_2\}_2]\text{BF}_4$  is at a lower frequency than other  $\text{AgS}_4$  species<sup>2</sup> and may indicate that on average less than four sulfur donors are coordinated per Ag ion in solution (only a single averaged

resonance would be expected due to fast exchange). The shifts in  $\delta(^{109}\text{Ag})$  to high frequency with added ligand and with decreasing temperature in  $[\text{Ag}\{o\text{-C}_6\text{H}_4(\text{SMe})_2\}_2]\text{BF}_4$  and  $[\text{Ag}\{o\text{-C}_6\text{H}_4(\text{TeMe})_2\}_2]\text{BF}_4$  are similar to those observed in other systems (although the actual  $\delta$ -value for the thioether systems is still lower than observed previously in complexes with  $\text{RSCH}_2\text{CH}_2\text{SR}$  ligands),<sup>2</sup> but  $[\text{Ag}\{o\text{-C}_6\text{H}_4(\text{SeMe})_2\}_2]\text{BF}_4$  is again anomalous (cf. the  $^{77}\text{Se}$  data above) in that, in the presence of excess  $o\text{-C}_6\text{H}_4(\text{SeMe})_2$ ,  $\delta(^{109}\text{Ag})$  shifts to low frequency. In the absence of observable spin–spin couplings the species present cannot be identified with certainty, but it may be that in the presence of excess ligand a species such as  $[\text{Ag}\{\eta^2\text{-}o\text{-C}_6\text{H}_4(\text{SeMe})_2\}\{\eta^1\text{-}o\text{-C}_6\text{H}_4(\text{SeMe})_2\}_2]\text{BF}_4$  may form (cf. the X-ray structure of the 1:2 complex).

## Conclusions

These studies of the *o*-phenylene-backboned group 16 ligands have revealed further the complexities in group 11 metal coordination chemistry. On the four objectives for this study delineated in the Introduction, three have been achieved to some extent and only the attempts to observe spin–spin couplings between  $^{107/109}\text{Ag}$  or  $^{63/65}\text{Cu}$  and  $^{77}\text{Se}$  or  $^{125}\text{Te}$  were unsuccessful. Coupling to the quadrupolar copper nuclei would only be expected under certain very specific conditions where the environment of the copper slowed the quadrupolar relaxation sufficiently. Couplings to the  $I = 1/2$  silver isotopes would be expected to be easier to observe but would be lost due to a fast-exchange process, and it is likely that, with high lability in group 16 ligand complexes of silver, a process such as reversible chelate ring opening is still significant even at low temperatures.

**Acknowledgment.** We thank the University of Southampton for support and the EPSRC for a grant to purchase the diffractometer.

**Supporting Information Available:** Tables of crystallographic data and refinement parameters, atomic coordinates, anisotropic thermal parameters, and complete bond lengths and angles for the three structures (15 pages). Ordering information is given on any current masthead page.

- (15) For a flattened tetrahedron  $[\text{Cu}(\text{L-L})_2]^+$  five NMR distinguishable invertomers are possible, although all may not be present in significant amounts. Four of the invertomers each have a single Te resonance since all the Te donors are symmetry related, while the fifth has four resonances each Te being distinct on symmetry grounds. (The problem is the same as the more familiar  $\text{trans-}[\text{M}(\text{L-L})_2\text{X}_2]$  case.) There is no way of predicting the relative abundances of the different invertomers. Inversion barriers increase  $\text{S} < \text{Se} < \text{Te}$  for a fixed metal system: Abel, E. W.; Orrell, K. G.; Scanlan, S. P.; Stevenson, D.; Kemmitt, T.; Levason, W. J. *Chem. Soc., Dalton Trans.* **1991**, 591.
- (16) Abel, E. W.; Bhargava, S. K.; Orrell, K. G. *Prog. Inorg. Chem.* **1984**, 32, 1.